Engineering Optimization

ISSN: 0305-215X (Print) 1029-0273 (Online) Journal homepage: www.tandfonline.com/journals/geno20

Fixture layout optimization of large compliant ship part assembly for reducing and straightening butt clearance

Ge Hong, Shuo Gao, Tangbin Xia, Juan Du, Xuancheng Jin, Ershun Pan & Lifeng Xi

To cite this article: Ge Hong, Shuo Gao, Tangbin Xia, Juan Du, Xuancheng Jin, Ershun Pan & Lifeng Xi (2024) Fixture layout optimization of large compliant ship part assembly for reducing and straightening butt clearance, Engineering Optimization, 56:9, 1473-1492, DOI: 10.1080/0305215X.2023.2258067

To link to this article: https://doi.org/10.1080/0305215X.2023.2258067

ENGINEERING OPTIMIZATION
2024, VOL. 56, NO. 9, 1473–1492
https://doi.org/10.1080/0305215X.2023.2258067

Taylor & Francis
Taylor & Francis Group

RESEARCH ARTICLE

Fixture layout optimization of large compliant ship part assembly for reducing and straightening butt clearance

Ge Hong[a], Shuo Gao[a], Tangbin Xia[a], Juan Du[b,c], Xuancheng Jin[a], Ershun Pan[a] and Lifeng Xi[a]

[a]State Key Laboratory of Mechanical System and Vibration, School of Mechanical Engineering, Shanghai Jiao Tong University, SJTU-Fraunhofer Center, Shanghai, People's Republic of China; [b]Smart Manufacturing Thrust, Systems Hub, The Hong Kong University of Science and Technology (Guangzhou), Guangzhou, China; [c]Guangzhou HKUST Fok Ying Tung Research Institute, Guangzhou, People's Republic of China

ABSTRACT

Fixture layout is an essential factor in intelligent manufacturing in the shipbuilding industry, affecting assembly quality and efficiency. Its optimization has become an urgent problem in the assembly process of compliant parts. Traditional fixture layout depends on workers' experience, which leads to butt clearance along the assembly interface. Thus, this article proposes a butt clearance control-oriented fixture layout optimization (BCCFLO) methodology. First, a method for calculating the part dimensional variation under the influence of fixture layout and fixture locating error is developed. Then, a constrained multi-objective integer nonlinear programming (CMINP) model is innovatively formulated to optimize the fixture layout. Furthermore, the non-dominated sorting genetic algorithm-II based on Latin hypercube sampling is designed to address the CMINP model. The case study illustrates and validates that the fixture layout achieved by the proposed method could significantly control the butt clearance for large compliant part assembly in the shipbuilding industry.

ARTICLE HISTORY
Received 18 February 2023
Accepted 7 September 2023

KEYWORDS
Compliant part assembly; fixture layout optimization; butt clearance control; finite element equation; large ship panels

1. Introduction

With the intense competition in the shipbuilding industry, manufacturers have been pursuing effective quality control and intelligent manufacturing to improve assembly quality and efficiency. Therefore, shipyards all over the world are motivated to improve the assembly quality of compliant parts to ensure the accuracy of ship construction with high efficiency (Eyres and Bruce 2012). In particular, the fixture layout significantly affects the dimensional variations of parts (Camelio, Hu, and Marin 2004; Phoomboplab and Ceglarek 2008). An appropriate fixture layout plays an important role in guaranteeing the geometric quality for the compliant part assembly process.

Based on the practical production process (Eyres and Bruce 2012; Liu *et al.* 2020), the general block construction process in the shipbuilding industry is shown in Figure 1. Owing to the large dimensions and compliant nature of ship parts (*e.g.* outer bottom plates), it is necessary to adjust fixtures (*e.g.* bed-jigs) in advance according to the layout, which is predetermined based on experiential knowledge. Then, the ship parts to be assembled are placed on the fixtures that have been adjusted. These processes are highlighted using the dashed frame in Figure 1.

However, because of the compliant nature of ship parts, the non-optimal predesigned fixture layout and fixture locating errors caused by manual adjustment, the parts are commonly deformed,

CONTACT Tangbin Xia xtbxtb@sjtu.edu.cn

Supplemental data for this article can be accessed online at https://doi.org/10.1080/0305215X.2023.2258067.

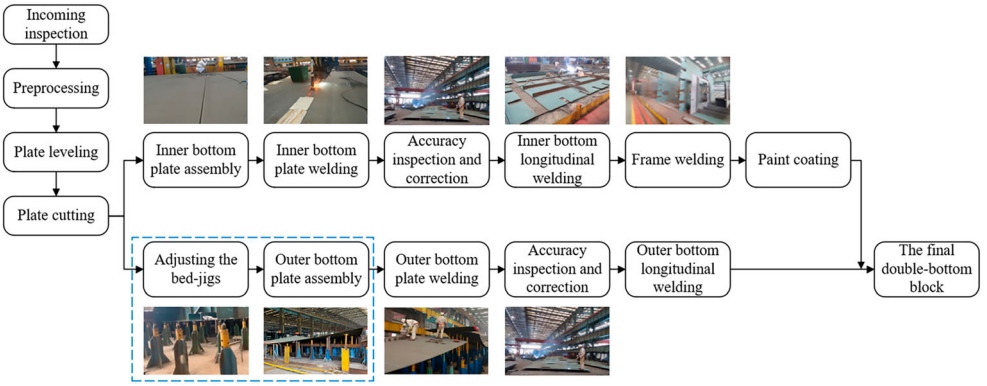

Figure 1. General block construction process in the shipbuilding industry.

which may result in the undesirable butt clearance of two compliant parts to be assembled. If the butt clearance is too large and uneven, it will be difficult to weld them together and will significantly influence the quality of the subsequent welding operation by introducing weld defects (Chen and Guedes Soares 2016). To satisfy the tolerance requirements before the subsequent welding process, surface treatments are required to reduce the butt clearance and make it uniform. However, these corrections are completed manually in the actual assembly process, which has a high cost and low efficiency, and is time consuming. Thus, this article mainly focuses on finding the optimal fixture layout, relying on computer-aided rather than artificial experience, which gives guidance for adjusting the fixtures to control the butt clearance along the assembly interface in the compliant part assembly process.

Previous research on fixture layout optimization can be divided into two categories, according to the mechanical nature of the parts. One category aims at optimizing the design of the fixture layout for rigid parts. For the single-station level, research has been conducted in the area of fixture layout design considering machining conditions. The genetic algorithm has been widely applied to optimize the fixture layout for minimizing geometric errors during the milling process (Kaya 2006) and avoiding positioning errors of the workpiece under machining loads (Butt *et al.* 2021). With the development of state-space modelling for multi-station assemblies, Kim and Ding (2004), Tian, Lai, and Lin (2009) and Xie *et al.* (2015) promoted fixture design optimization from single-station to multi-station systems. The above methods are all suitable for the fixture layout optimization of rigid parts, but cannot be directly used for compliant parts.

The other category concentrates on fixture layout optimization for non-rigid parts. Earlier research on the fixture design of compliant workpieces used finite element analysis (FEA) to calculate part deformation (Cai, Hu, and Yuan 1996; Xing 2017). To improve the optimization efficiency, surrogate models for replacing the FEA have been established. Yang *et al.* (2017) proposed a kriging-based model to evaluate the numerical relationship between the fixture layout and the corresponding part deformation. Nevertheless, the surrogate model significantly depends on the training and testing data sets generated from FEA simulations. Du *et al.* (2021) proposed a physics-driven model from first principles to calculate the nodal displacement under different fixture layouts without using intensive FEA simulations, although the locating error of the fixture was not considered.

Since variations will always exist, researchers have also studied fixture layout optimization problems in the stochastic environment. Several approaches have been developed to find the optimal fixture layout for a '3-2-1' locating scheme to minimize the part variations considering fixture positions and fixture variations (Camelio, Hu, and Ceglarek 2004; Li *et al.* 2008). Vishnupriyan, Majumder, and Ramachandran (2011) used a finite element method and a genetic algorithm to optimize fixture layouts considering the effects of workpiece positional errors, elastic deformation and

machining errors. The current literature on fixture layout optimization mainly aims to minimize the part deformation of individual parts (Cai, Hu, and Yuan 1996; Yang *et al.* 2017; Xing 2017). However, there is a lack of a fixture layout optimization method for the '*N*-2-1' locating principle that controls the butt clearance of compliant ship parts to be assembled in the presence of fixture locating errors.

Motivated by this research gap and the assembly process of real-world compliant ship panels, this article proposes a butt clearance control-oriented optimization of fixture layout for large compliant part assembly. The contributions of this article can be summarized as follows:

(1) The butt clearance control-oriented fixture layout optimization (BCCFLO) method, which considers reducing and straightening the butt clearance for fixture layout optimization in the assembly process of compliant ship parts, is proposed for the first time.
(2) A modified finite element equation considering fixture layout and fixture locating error (FEE-FLE) for calculating nodal displacement is proposed for fixture layout optimization. The FEE-FLE method can be directly applied to calculate part deformation under fixture layouts and locating errors, rather than intensive FEA simulations.
(3) The fixture layout optimization problem is formulated as a constrained multi-objective integer nonlinear programming (CMINP) model, considering the practical production environment. This model focuses on controlling the butt clearance under practical constraints. The non-dominated sorting genetic algorithm-II based on Latin hypercube sampling (NSGA-II-LHS) is proposed for solving the proposed CMINP model.

The remainder of this article is organized as follows. Section 2 describes the fixture layout optimization problem in the assembly process of compliant ship panels, and presents the flowchart of the proposed BCCFLO method. Section 3 describes the proposed FEE-FLE method and the mathematical formulation of the CMINP model. Section 4 presents the NSGA-II-LHS method for solving the CMINP model to obtain the optimal fixture layout. Then, a case study illustrating the effectiveness of the proposed method on fixture layout optimization for the assembly process of curved panels in the shipbuilding industry is introduced in Section 5. Finally, Section 6 draws conclusions and provides further perspective.

2. Problem statement

2.1. Problem description

To reduce the deformation caused by gravity, the '*N*-2-1' ($N \geq 3$) locating principle is widely used as an overconstraint condition to locate and support sheet metal parts. As shown in Figure 2(a) and (b), there are *N*, 2 and 1 points for supporting the part on the primary datum, the secondary datum and the tertiary datum, respectively. The quantity of fixtures placed on the primary datum is a predetermined parameter (Cai, Hu, and Yuan 1996; Yang *et al.* 2017; Du *et al.* 2021) according to the specific parts in the design phase. The fixture can be adjusted in the *x*-, *y*- and *z*-directions to hold the part in the desired position (Shen *et al.* 2020). However, the fixture may deviate from the ideal position, which further deforms the parts.

Using P_i as an example, the variations in the *x*-, *y*- and *z*-directions can be denoted as $(\Delta x_i,\ \Delta y_i,\ \Delta z_i)$. In the actual production process, fixtures can be fixed accurately in the corresponding positions in the *x*–*y* plane. Then, workers manually adjust fixtures in the *z*-direction, which will lead to potential fixture variations Δz_i in the height direction, as shown in Figure 3. The influences of Δx_i and Δy_i on dimensional variations can be neglected, whereas Δz_i, indicating the locating error between the nominal position and the actual position in the *z*-direction, plays an important role in the part deformation (Rong *et al.* 2001). Therefore, it is necessary to consider the influence of the Δz_i, representing the fixture locating error on the part deformation.

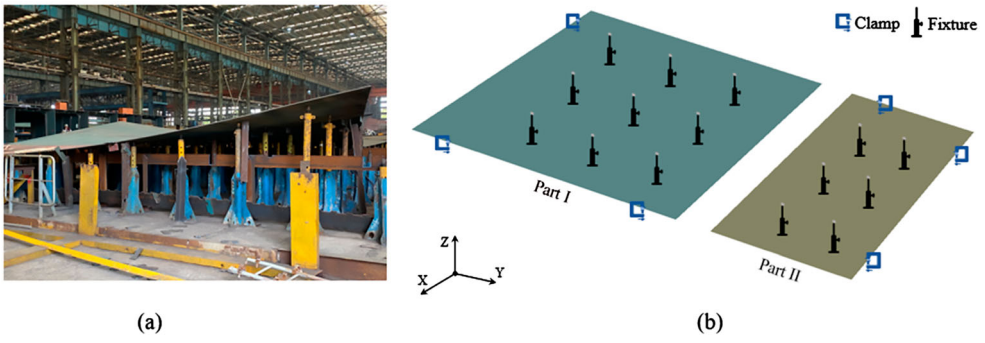

Figure 2. Compliant part assembly based on the '*N*-2-1' locating principle: (a) actual production environment; (b) simulation model.

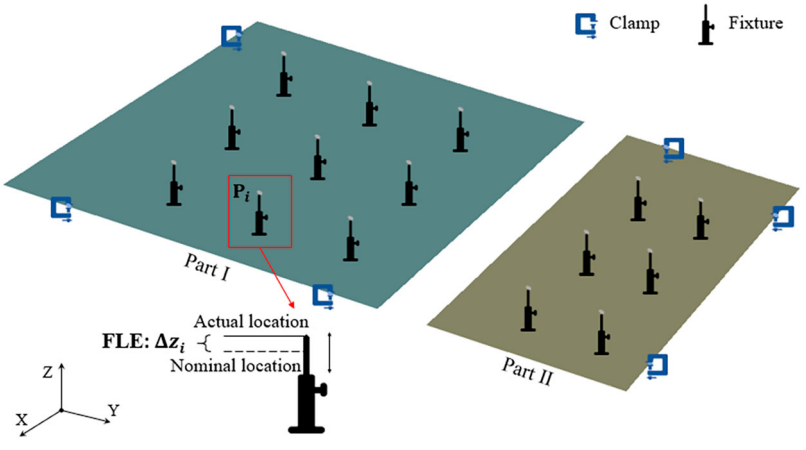

Figure 3. Fixture locating error (FLE) in the '*N*-2-1' locating principle.

Overall, the main purpose of this article is to find the optimal fixture layout considering the fixture locating error to control the butt clearance along the assembly interface during the compliant part assembly process.

To formulate the mathematical model of the fixture layout optimization problem, the following assumptions are made, based on the practical assembly process of compliant parts:

(1) The fixture locating error in the z-direction is considered.
(2) The part is considered an ideal part before the assembly process, regardless of part variations due to part processing.
(3) The number of fixtures is given, and the fixture sequence is not considered according to practical experience.

2.2. Framework for fixture layout optimization

In the butt clearance control-oriented optimization of fixture layout, the main process of BCCFLO is required to output the optimal fixture layout by formulating the FEA model, calculating nodal displacement, and establishing and solving the CMINP model. An overview of the proposed method is shown in Figure 4.

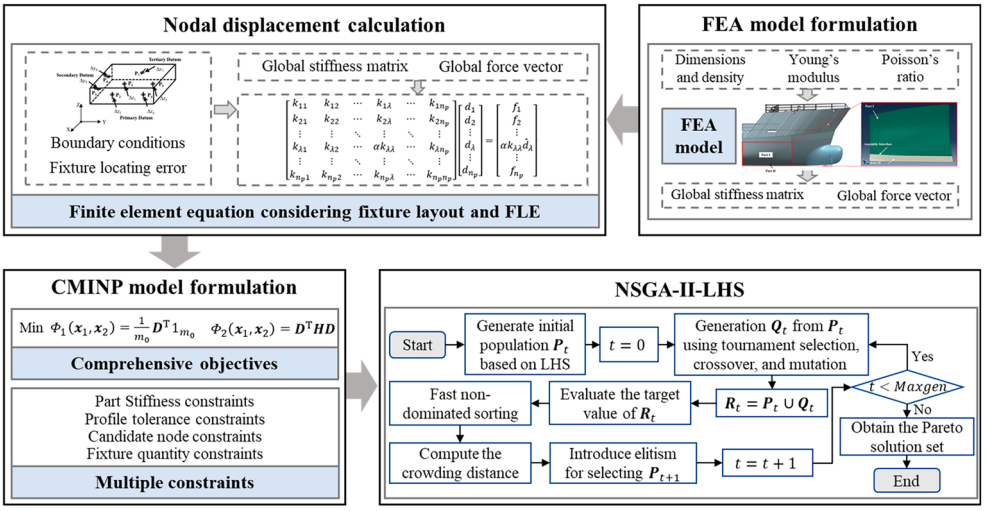

Figure 4. Flowchart of the butt clearance control-oriented fixture layout optimization (BCCFLO) method for optimizing fixture layout. FLE = fixture locating error; FEE = finite element equation; CMINP = constrained multi-objective integer nonlinear programming; NSGA-II-LHS = non-dominated sorting genetic algorithm-II based on Latin hypercube sampling; LHS = Latin hypercube sampling.

First, the FEA model is established to export the global stiffness matrix **K** and the global force vector **f**. The FEE-FLE using the modified **K** and **f** is proposed to calculate the nodal displacements, given the fixture layout and fixture locating errors. Then, the CMINP model is formulated to control the butt clearance while satisfying multiple constraints. The mathematical notations are shown in Table 1 in the supplementary material. Finally, the NSGA-II-LHS method is designed for solving the CMINP model and further obtaining the optimal fixture layout.

3. Model formulation

3.1. FEA model formulation

To develop the FEA model, the physical entity of the part is meshed into discrete component elements and nodes that can be solved by a computer, as shown in Figure 5. Consider that a meshed compliant part p ($p = 1, 2$) has m_p nodal points and n_p ($n_p = m_p \times df$) nodal displacements, where $df = 6$ is the degree of freedom for each node. Each node has a node label; let $\mathcal{M}_p = \{1, \cdots, m_p\}$ be the set of all node labels of part p, and $\text{card}(\mathcal{M}_p) = m_p$.

The FEA is a widely used approach for calculating the nodal displacements of plates by subdividing the continuum into finite elements. Once the FEA model has been established, **K** and **f** are exported through the commercial FEA solver. Finally, the solution of nodal displacements is calculated by the following finite element equation (FEE):

$$\mathbf{K}\boldsymbol{d} = \mathbf{f} \tag{1}$$

Taking part p as an example, **K** is an $n_p \times n_p$ matrix. For each mesh node of part p, the nodal displacement vector $\boldsymbol{d}^i = [d_x^i; d_y^i; d_z^i; \omega_x^i; \omega_y^i; \omega_z^i], i \in \{1, \cdots, m_p\}$ and the nodal force vector $\mathbf{f}^i = [f_x^i; f_y^i; f_z^i; \tau_x^i; \tau_y^i; \tau_z^i], i \in \{1, \cdots, m_p\}$. Then, both $\boldsymbol{d} = [\boldsymbol{d}^1; \cdots; \boldsymbol{d}^i; \cdots; \boldsymbol{d}^{m_p}]$ and $\mathbf{f} = [\mathbf{f}^1; \cdots; \mathbf{f}^i; \cdots; \mathbf{f}^{m_p}]$ are $n_p \times 1$ vectors, by aggregating the nodal displacement vector and the nodal

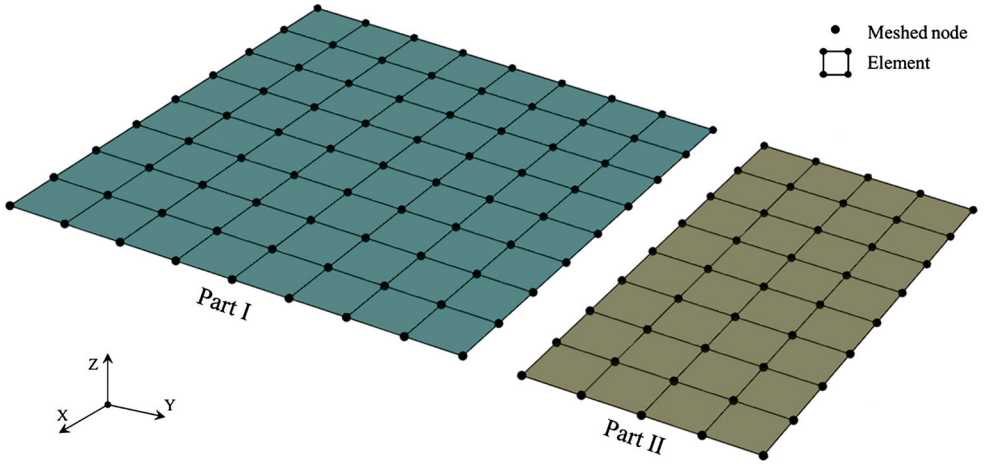

Figure 5. Parts meshed into discrete nodes and elements.

force vector, respectively. The full matrix form of Equation (1) can be expressed as follows:

$$\begin{bmatrix} k_{11} & k_{12} & k_{13} & \cdots & k_{1n_p} \\ k_{21} & k_{22} & k_{23} & \cdots & k_{2n_p} \\ \vdots & \vdots & \vdots & \ddots & \vdots \\ k_{n_p1} & k_{n_p2} & k_{n_p3} & \cdots & k_{n_pn_p} \end{bmatrix} \begin{bmatrix} d_1 \\ d_2 \\ \vdots \\ d_{n_p} \end{bmatrix} = \begin{bmatrix} f_1 \\ f_2 \\ \vdots \\ f_{n_p} \end{bmatrix} \tag{2}$$

However, Equation (2) cannot be solved directly because of the singularity of **K**. Thus, the displacement boundary constraints imposed by physical support must be introduced to eliminate the singularity of **K**. The fixture is one kind of physical support, which means that placing fixtures is equivalent to implementing displacement boundary conditions.

3.2. Nodal displacement calculation by FEE-FLE

In this section, a new modified FEE considering FLE is proposed for the nodal displacement calculation in the fixture layout optimization problem. Both the fixture layout and the FLE are considered, and their influences on the static part response are captured by implementing the displacement boundary conditions. Figure 6 shows the flowchart of the proposed procedure of FEE-FLE to impose boundary conditions.

Step 1: Determine the position of the constraint in **K** and **f**. The indicator variables are used to link the fixture layouts to the boundary conditions.
Step 2: Determine whether it is a non-zero displacement boundary condition. If the constraint is imposed by the clamp, the displacement boundary condition imposed on the node is zero, then turn to Step 3 to modify **K** and **f**. If the constraint is imposed by the fixture, the FLE is considered as a non-zero displacement boundary condition, then turn to Step 4 to modify **K** and **f**.
Step 3: Modification under zero displacement boundary condition. The constraint imposed by the clamp is along the x-direction or y-direction, then $\gamma = 6(u-1)+1$ or $\gamma = 6(u-1)+2$, respectively. Taking the clamp placed on P_u as an example (u is the node label), keep the γth diagonal element unchanged and set $f_\gamma = k_{\gamma e} = 0$ for $e = 1, 2, \cdots, \gamma-1, \gamma+1, \cdots, n_p$. Thus,

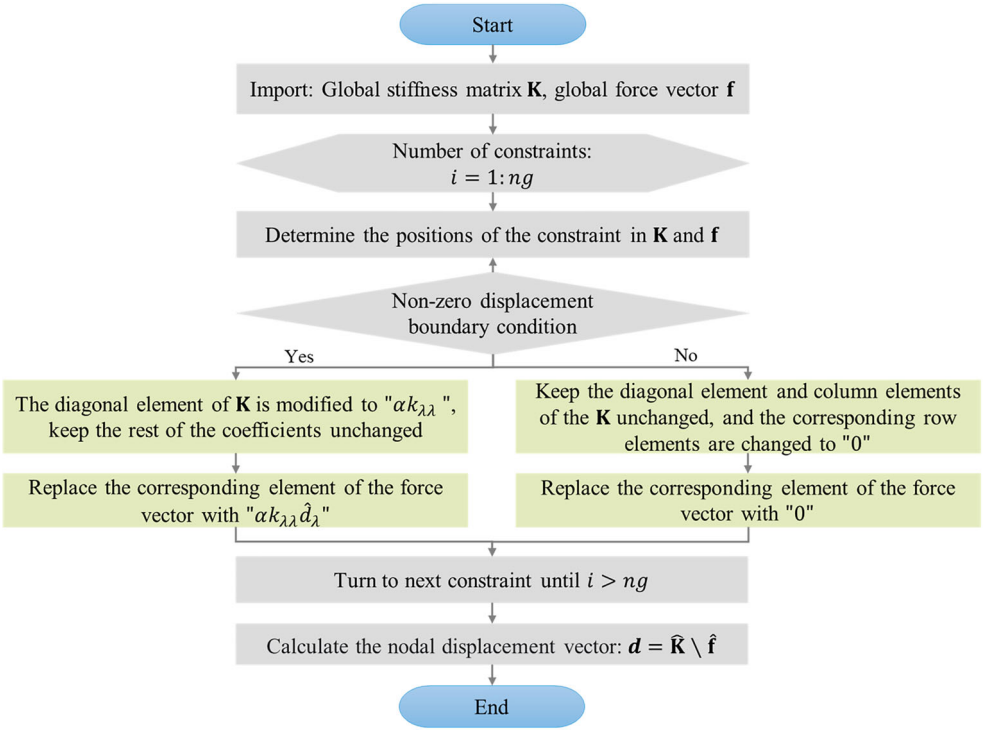

Figure 6. Flowchart of the proposed procedure for modifying the finite element equation (FEE).

the modification of Equation (1) under the zero displacement boundary condition is defined by:

$$\begin{bmatrix} k_{11} & k_{12} & \cdots & k_{1\gamma} & \cdots & k_{1n_p} \\ k_{21} & k_{22} & \cdots & k_{2\gamma} & \cdots & k_{2n_p} \\ \vdots & \vdots & \ddots & \vdots & \ddots & \vdots \\ 0 & 0 & \cdots & k_{\gamma\gamma} & \cdots & 0 \\ \vdots & \vdots & \ddots & \vdots & \ddots & \vdots \\ k_{n_p1} & k_{n_p2} & \cdots & k_{n_p\gamma} & \cdots & k_{n_pn_p} \end{bmatrix} \begin{bmatrix} d_1 \\ d_2 \\ \vdots \\ d_\gamma \\ \vdots \\ d_{n_p} \end{bmatrix} = \begin{bmatrix} f_1 \\ f_2 \\ \vdots \\ 0 \\ \vdots \\ f_{n_p} \end{bmatrix} \tag{3}$$

Step 4: Modification under non-zero displacement boundary condition. Taking the fixture placed on P_σ as an example (σ is the node label), suppose $\lambda = 6(\sigma - 1) + 3$. Firstly, multiply the diagonal element of **K** corresponding to the node to which the boundary condition is applied by a large number α ($\alpha \gg k_{\lambda e}, e = 1, 2, \cdots, \lambda - 1, \lambda + 1, \cdots, n_p$), and keep the rest of the coefficients unchanged. Secondly, replace the corresponding element of **f** with the product of $\alpha k_{\lambda\lambda}$ and the specified value of the FLE. Suppose that the FLE of the fixture $\hat{d}_\lambda = \Delta z_\sigma$ is given. Δz_σ denotes the FLE of the corresponding fixture placed on P_σ. Then, the λth equation modified from Equation (1) is:

$$\sum_{e=1, e\neq\lambda}^{n_p} k_{\lambda e} d_e + \alpha k_{\lambda\lambda} d_\lambda = f_\lambda - k_{\lambda\lambda}\hat{d}_\lambda + \alpha k_{\lambda\lambda}\hat{d}_\lambda \approx \alpha k_{\lambda\lambda}\hat{d}_\lambda \tag{4}$$

Then, the full matrix form can be expressed as follows:

$$\begin{bmatrix} k_{11} & k_{12} & \cdots & k_{1\lambda} & \cdots & k_{1n_p} \\ k_{21} & k_{22} & \cdots & k_{2\lambda} & \cdots & k_{2n_p} \\ \vdots & \vdots & \ddots & \vdots & \ddots & \vdots \\ k_{\lambda 1} & k_{\lambda 2} & \cdots & \alpha k_{\lambda\lambda} & \cdots & k_{\lambda n_p} \\ \vdots & \vdots & \ddots & \vdots & \ddots & \vdots \\ k_{n_p 1} & k_{n_p 2} & \cdots & k_{n_p\lambda} & \cdots & k_{n_p n_p} \end{bmatrix} \begin{bmatrix} d_1 \\ d_2 \\ \vdots \\ d_\lambda \\ \vdots \\ d_{n_p} \end{bmatrix} = \begin{bmatrix} f_1 \\ f_2 \\ \vdots \\ \alpha k_{\lambda\lambda} \hat{d}_\lambda \\ \vdots \\ f_{n_p} \end{bmatrix} \tag{5}$$

Step 5: Identify whether all the constraints are imposed or not. If no, turn to Step 2 to determine whether the displacement boundary condition is non-zero. If yes, suppose that the modified global stiffness matrix is $\hat{\mathbf{K}}$ and the modified global force vector is $\hat{\mathbf{f}}$, then the final nodal displacement is calculated through $\hat{\mathbf{K}}\boldsymbol{d} = \hat{\mathbf{f}}$.

3.3. CMINP model formulation

According to the problem description and FEA model formulation detailed in Sections 2.1 and 3.1, respectively, this section develops a multi-objective integer nonlinear programming model for fixture layout optimization.

3.3.1. CMINP variables

This article uses meshed nodes in FEA on the part as candidate locating points for the fixtures to be placed. Suppose that $\boldsymbol{\mathcal{M}}_p$ consists of the meshed node labels on part p, and $m = \text{card}(\boldsymbol{\mathcal{M}}_1) + \text{card}(\boldsymbol{\mathcal{M}}_2) = m_1 + m_2$. Let $\boldsymbol{\mathcal{M}}_p^{\text{F}}$ ($\boldsymbol{\mathcal{M}}_p^{\text{F}} \subseteq \boldsymbol{\mathcal{M}}_p$) be the set of potential feasible nodes labels on part p for placing fixtures and $\text{card}(\boldsymbol{\mathcal{M}}_p^{\text{F}}) = m_p^{\text{F}}$. Therefore, the purpose of the fixture layout optimization problem is to determine the set of N fixture locating nodes, denoted as $\boldsymbol{\mathcal{M}}^{\text{CN}}$, from the set $\boldsymbol{\mathcal{M}}^{\text{F}}$ ($\boldsymbol{\mathcal{M}}^{\text{F}} = \boldsymbol{\mathcal{M}}_1^{\text{F}} \cup \boldsymbol{\mathcal{M}}_2^{\text{F}}$), consisting of m^{F} ($m^{\text{F}} = m_1^{\text{F}} + m_2^{\text{F}}$) potential feasible node on two parts, where N is a known constant. Let $\boldsymbol{x}_p = \{x_p^1, \cdots, x_p^i, \cdots, x_p^{m_p}\}$, $x_p^i \in \{0, 1\}$ represent the decision variables; $x_p^i = 0$ indicates that there is a fixture placed at the node label i on part p, $i \in \boldsymbol{\mathcal{M}}_p = \{1, \cdots, m_p\}$. m_0 is the number of meshed nodes in FEA along the assembly interface.

3.3.2. Constraints

Since the CMINP model is based on the FEE-FLE, the part stiffness constraints need to be included. In addition, in the actual compliant part assembly process, practitioners expect that the surface profile tolerances of compliant parts will meet the precision requirements. Not all nodes are suitable for placing fixtures, and the number of fixtures is predetermined. Thus, it is necessary to add constraints of part stiffness, profile tolerance, feasible fixture positioning points and fixture quantity to the CMINP model.

3.3.2.1. Part stiffness constraints. $\hat{\mathbf{K}}_p(\boldsymbol{x}_p)$ and $\hat{\mathbf{f}}_p(\boldsymbol{x}_p, \boldsymbol{d}_p^{\text{FLE}})$ are defined as the modified global stiffness matrix and global force vector in the FEE-FLE, according to Section 3.2. $N_p = m_p - \parallel \boldsymbol{x}_{p_0} \parallel_0$ is defined as the number of fixtures on part p. $\boldsymbol{d}_p^{\text{FLE}} = \{\Delta z_1, \Delta z_2, \cdots, \Delta z_{N_p}\}$ represents the FLE of fixtures placed on part p. Thus, the stiffness constraints of the two parts are shown by the following equations:

$$\hat{\mathbf{K}}_p(\boldsymbol{x}_p)\boldsymbol{d}_p = \hat{\mathbf{f}}_p(\boldsymbol{x}_p, \boldsymbol{d}_p^{\text{FLE}}), p = 1, 2 \tag{6}$$

3.3.2.2. Profile tolerance constraints. The ith nodal displacement of part p that denotes the surface profile tolerance is $\| (\boldsymbol{d}_p^i)^{\mathrm{T}} \boldsymbol{W} \|_2$, where $\boldsymbol{d}_p^i = [d_{xp}^i; d_{yp}^i; d_{zp}^i; \omega_{xp}^i; \omega_{yp}^i; \omega_{zp}^i], i = 1, 2, \cdots, m_p$ and $\mathrm{diag}(\boldsymbol{W}) = [1, 1, 1, 0, 0, 0]^{\mathbf{T}}$. Practitioners will expect the nodal displacement to satisfy the practical accuracy requirement ε during the actual compliant part assembly process. Then, the profile tolerance constraints of the two parts can be expressed as:

$$\| (\boldsymbol{d}_p^i)^{\mathrm{T}} \boldsymbol{W} \|_2 \leq \varepsilon,\ i = 1, 2, \cdots, m_p,\ p = 1,\ 2 \tag{7}$$

3.3.2.3. Candidate node constraints. In the actual assembly process shown in Figure 2(a), fixtures and clamps cannot be placed on the nodes along the assembly interface. According to the 'N-2-1' locating principle and practical assembly process, the nodes on the boundaries are infeasible, while the nodes on the primary datum are feasible for placing fixtures, as shown in Figure 7. Let $\bar{\boldsymbol{\mathcal{M}}}_p^{\mathrm{F}}$ represent the supplementary set of $\boldsymbol{\mathcal{M}}_p^{\mathrm{F}}$, *i.e.* $\bar{\boldsymbol{\mathcal{M}}}_p^{\mathrm{F}} = \boldsymbol{\mathcal{M}}_p \setminus \boldsymbol{\mathcal{M}}_p^{\mathrm{F}}$, and $\mathrm{card}(\bar{\boldsymbol{\mathcal{M}}}_p^{\mathrm{F}}) = \bar{m}_p^{\mathrm{F}}$. This implies that $\bar{\boldsymbol{\mathcal{M}}}_p^{\mathrm{F}}$ contains all nodes on part p at which fixtures cannot be placed. Thus, the constraints on infeasible fixture locating points can be enforced by the following equations:

$$x_p^j = 1,\ j \in \bar{\boldsymbol{\mathcal{M}}}_p^{\mathrm{F}},\ p = 1,\ 2 \tag{8}$$

3.3.2.4. Fixture quantity constraints. Let N equal the total quantity of the fixtures to be placed on the primary datum plane. Concerning the CMINP model, this implies that N number of candidate nodes is activated for placing fixtures. This will occur if N number of x_p^i variables are zeros. The sets of activated candidate nodes for each part are defined as $\boldsymbol{\mathcal{M}}_1^{\mathrm{CN}}$ and $\boldsymbol{\mathcal{M}}_2^{\mathrm{CN}}$. Thus, this restriction on the number of candidate nodes for imposing fixtures can be achieved with the following constraints:

$$x_p^c = 0, x_p^g = 1, c \in \boldsymbol{\mathcal{M}}_p^{\mathrm{CN}}, g \in \boldsymbol{\mathcal{M}}_p^{\mathrm{F}} \setminus \boldsymbol{\mathcal{M}}_p^{\mathrm{CN}}, p = 1,\ 2 \tag{9}$$

$$\| \boldsymbol{x}_1 \|_0 + \| \boldsymbol{x}_2 \|_0 = m - N \tag{10}$$

3.3.3. Objective functions

In the actual compliant part assembly process, practitioners aim to control the butt clearance in order to reduce trimming or correction before the welding operation. The main purpose of this article is to optimize the fixture layout to guide the fixture adjusting process. The influence of part deformation on the dimensional gaps and assembly interface straightness is quantified by the mean and variance

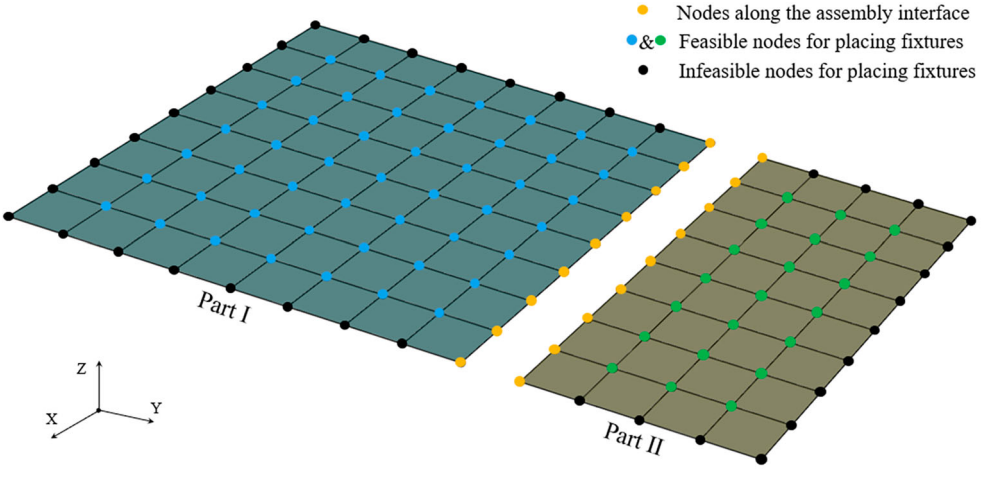

Figure 7. Illustration of nodes along the assembly interface, feasible and infeasible nodes for placing fixtures.

of the Euclidean distance among each pair of nodes at the assembly edge, respectively. The objective functions of the optimization model can be formulated mathematically as follows:

$$\Phi_1(\boldsymbol{x}_1, \boldsymbol{x}_2) = (\boldsymbol{D}^{\mathrm{T}} 1_{m_0})/m_0 \tag{11}$$

$$\Phi_2(\boldsymbol{x}_1, \boldsymbol{x}_2) = \boldsymbol{D}^{\mathrm{T}} \boldsymbol{H} \boldsymbol{D} \tag{12}$$

$\Phi_1(\boldsymbol{x}_1, \boldsymbol{x}_2)$ and $\Phi_2(\boldsymbol{x}_1, \boldsymbol{x}_2)$ are the objective functions of the CMINP model, representing closing the dimensional gaps and improving the straightness of the assembly clearance, respectively. $1_{m_0} = (1; 1; \cdots; 1)_{m_0 \times 1}$, $\boldsymbol{H} = \boldsymbol{I}_{m_0} - (1/m_0) 1_{m_0} 1_{m_0}{}^{\mathrm{T}}$. Let $\boldsymbol{\mathcal{M}}_1^{\mathrm{AI}}$ and $\boldsymbol{\mathcal{M}}_2^{\mathrm{AI}}$ represent the set of node labels along the assembly interface of parts I and II, $\mathrm{card}(\boldsymbol{\mathcal{M}}_1^{\mathrm{AI}}) = \mathrm{card}(\boldsymbol{\mathcal{M}}_2^{\mathrm{AI}}) = m_0$. Suppose that node $\mu \in \boldsymbol{\mathcal{M}}_1^{\mathrm{AI}}$ on part I and the corresponding node $\nu \in \boldsymbol{\mathcal{M}}_2^{\mathrm{AI}}$ on part II form a node pair ξ; the Euclidean distance between node μ and node ν is defined as $D_\xi = \sqrt{(\boldsymbol{d}_1^\mu - \boldsymbol{d}_2^\nu)^{\mathrm{T}} \boldsymbol{W} (\boldsymbol{d}_1^\mu - \boldsymbol{d}_2^\nu)}$. Then, the vector of all Euclidean distances is defined as $\boldsymbol{D} = [D_1, \cdots, D_\xi, \cdots, D_{m_0}]$.

In conclusion, the mathematical formulation of the optimization model can be written as follows:

$$\begin{aligned}
Min \quad & \Phi_1(\boldsymbol{x}_1, \boldsymbol{x}_2) = (\boldsymbol{D}^{\mathrm{T}} 1_{m_0})/m_0 \\
& \Phi_2(\boldsymbol{x}_1, \boldsymbol{x}_2) = \boldsymbol{D}^{\mathrm{T}} \boldsymbol{H} \boldsymbol{D} \\
\text{Subject to} \quad & \hat{\mathbf{K}}_p(\boldsymbol{x}_p) \boldsymbol{d}_p = \hat{\mathbf{f}}_p(\boldsymbol{x}_p, \boldsymbol{d}_p^{\mathrm{FLE}}), p = 1,\ 2 \\
& \parallel (\boldsymbol{d}_p^i)^{\mathrm{T}} \boldsymbol{W} \parallel_2 \leq \varepsilon, i = 1, 2, \cdots, m_p, p = 1,\ 2 \\
& x_p^j = 1,\ j \in \bar{\boldsymbol{\mathcal{M}}}_p^{\mathrm{F}}, p = 1,\ 2 \\
& x_p^c = 0, x_p^g = 1, c \in \boldsymbol{\mathcal{M}}_p^{\mathrm{CN}}, g \in \boldsymbol{\mathcal{M}}_p^{\mathrm{F}} \setminus \boldsymbol{\mathcal{M}}_p^{\mathrm{CN}}, p = 1,\ 2 \\
& \parallel \boldsymbol{x}_1 \parallel_0 + \parallel \boldsymbol{x}_2 \parallel_0 = m - N
\end{aligned} \tag{13}$$

4. Implementation of the NSGA-II-LHS for the CMINP model

According to the CMINP model, a non-dominated sorting genetic algorithm-II based on Latin hypercube sampling (NSGA-II-LHS) is developed. The specific procedure of the NSGA-II-LHS method is presented in Table 1.

The non-dominated sorting genetic algorithm-II (NSGA-II) has been used successfully to obtain Pareto-optimal solutions for multi-objective problems (Shojaeefard *et al.* 2018; Xu, Jiang, and Pueh

Table 1. Non-dominated sorting genetic algorithm-II based on Latin hypercube sampling (NSGA-II-LHS) method for solving the constrained multi-objective integer nonlinear programming (CMINP) model.

Algorithm 1. NSGA-II-LHS method

Input: Fixture quantity: *N*; population size: *L*; maximum generation: *Maxgen*
Output: Pareto-optimal solutions of the fixture layout
1. Initialize: Produce an initial population $\boldsymbol{P}_0$ including *L* number of fixture layouts $\boldsymbol{x}_0$ through LHS and random generation
2. **For** $t = 0, 1, \cdots, Maxgen$ **do**
3. Generate an offspring population $\boldsymbol{Q}_t$ of size *L* from $\boldsymbol{P}_t$ using tournament selection, crossover and mutation
4. $\boldsymbol{R}_t = \boldsymbol{P}_t \cup \boldsymbol{Q}_t$
5. Compute $\Phi_1(\boldsymbol{x})$ and $\Phi_2(\boldsymbol{x})$ of $\boldsymbol{x} \in \boldsymbol{R}_t$ given the nodal displacements calculated by FEE-FLE
6. Calculate the non-dominated fronts of $\boldsymbol{R}_t$:$(\boldsymbol{\mathcal{F}}_1, \boldsymbol{\mathcal{F}}_2, \cdots, \boldsymbol{\mathcal{F}}_i, \cdots)$ = fast - non - dominated - sort $(\boldsymbol{R}_t)$
7. $\boldsymbol{P}_{t+1} = \emptyset$ and $\xi = 1$
8. **Repeat**
9. Compute the crowding distance in $\boldsymbol{\mathcal{F}}_\xi$
10. Sort $\boldsymbol{\mathcal{F}}_\xi$ in descending order using the crowded-comparison operator
11. $\boldsymbol{P}_{t+1} = \boldsymbol{P}_{t+1} \cup \boldsymbol{\mathcal{F}}_\xi[1 : (L - |\boldsymbol{P}_{t+1}|)]$
12. $\xi = \xi + 1$
13. **Until** $|\boldsymbol{P}_{t+1}| + |\boldsymbol{\mathcal{F}}_\xi| \leq L$
14. $t = t + 1$
15. **End for**

Note: LHS = Latin hypercube sampling; FEE-FLE = finite element equation considering fixture layout and fixture locating error.

Lee 2017). Although it does not ensure that all objectives are optimal simultaneously, NSGA-II leads to Pareto-optimal solutions by compromising among multiple objective functions. In the following subsections, the problem-specific population initialization, crossover and mutation strategies, as well as the constraint handling method, are described.

4.1. Population initialization

The quality of the initial population has a great influence on the results of the algorithm. According to the characteristics of decision variables introduced in Section 3.3.1, 0–1 binary encoding is adopted.

In this article, the number of genes in a chromosome is equal to m. To satisfy constraint (8), set $x_p^i = 1,\ i \in \bar{\mathcal{M}}_p^{\mathrm{F}}$, which means that x_p^i is fixed. Then, N nodes are randomly selected from the remaining m^{F} feasible nodes. To avoid the concentration of selected nodes, Latin hypercube sampling (LHS) (McKay, Beckman, and Conover 2000) is adopted to generate a fraction of the initial population. LHS operates by dividing the space of $\mathcal{M}^{\mathrm{F}}$ into N disjoint subsets with equal probability. Then, a node label is randomly selected from each subset to form a new $\mathcal{M}^{\mathrm{CN}}$. Set $x_p^c = 0$, for c in the new $\mathcal{M}^{\mathrm{CN}}$; $x_p^g = 1,\ g \in \mathcal{M}^{\mathrm{F}} \setminus \mathcal{M}^{\mathrm{CN}}$. Compared with simple random generation, the population obtained by both LHS and random generation has better randomness, uniformity and diversity.

4.2. Crossover and mutation strategies

Crossover and mutation are two common types of stochastic transformation method for generating new chromosomes in genetic operators. In this article, partially matched crossover (PMX) (Chan and Tansri 1994) is adapted to produce child chromosomes. The purpose of the CMINP model is to select N nodes from m^{F} ($N \ll m^{\mathrm{F}}$) feasible nodes, which means that the number of zeros in the chromosome is less than the number of ones. If the crossover strategy is applied directly to parent chromosomes, the child chromosome is likely to be the same as the parent chromosome. To avoid this phenomenon, the corresponding node labels where the fixtures are placed are used as the sequences to be crossed. Since the fixture cannot be repeatedly placed at the same node, the PMX is adapted because it ensures that genes in each sequence appear only once.

Mutation randomly modifies one or more allele genes in an individual chromosome to escape from the local optimum. A random number is generated from the interval [0,1] and compared with the preset mutation rate. In the case of a binary string, if the random number is less than or equal to the mutation rate, the randomly selected gene is changed from 0 to 1, or *vice versa*. To satisfy the defined constraint (10), it is necessary to perform another bit-flip mutation to ensure that the number of zeros in the chromosome is N.

4.3. Constraint handling method

This article uses the constraint handling method proposed by Deb *et al.* (2002). The CMINP model has the profile tolerance constraint for two parts. The constraint is quantified as whether each nodal displacement is within the accuracy requirement. To determine two infeasible solutions in which one violates more constraints than the other, an indicator function is defined for each node as follows:

$$\delta^i(\boldsymbol{x}_1, \boldsymbol{x}_2) = \begin{cases} 1, & \text{If } C_1 \text{ or } C_2 \text{ is not satisfied} \\ 0, & \text{If both } C_1 \text{ and } C_2 \text{ are satisfied} \end{cases} \tag{14}$$

$$C_1 = \{\boldsymbol{x}_1 : \parallel (\boldsymbol{d}_1^i)^{\mathrm{T}} \boldsymbol{W} \parallel_2 \leq \varepsilon,\ i \in \mathcal{M}_1\}$$

$$C_2 = \{\boldsymbol{x}_2 : \parallel (\boldsymbol{d}_2^i)^{\mathrm{T}} \boldsymbol{W} \parallel_2 \leq \varepsilon,\ i \in \mathcal{M}_2\}$$

The violation for the whole nodal displacement is calculated as follows:

$$\Delta(\delta^i) = \sum_{i \in \mathcal{M}_1 \cup \mathcal{M}_2} \delta^i(\boldsymbol{x}_1, \boldsymbol{x}_2) \tag{15}$$

5. Case study

In this section, the assembly process of two compliant parts (outer bottom plates) in the shipbuilding industry is analysed to demonstrate the effectiveness of the proposed method for fixture layout optimization considering the FLE.

5.1. Model parameters

This article focuses on the assembly process of two compliant parts in the shipbuilding industry, such as the outer bottom plate assembly process in Figure 1. Part I is a curved panel with different curvature radii. The lengths of the four sides are 5600, 4600, 5500 and 3200 mm. Part II is an approximate rectangle with a length of 5500 mm and a width of 600 mm. The thickness of the parts is 6 mm. The Young's modulus, Poisson's ratio and density of the parts are 210,000 N/mm^2, 0.3 and 7.85×10^{-3} g/mm^3, respectively.

In the actual production process, the height of each supporting fixture under the part is highly dependent on manual adjustment. Hence, there are inevitable locating errors of the fixtures in the z-direction. The height tolerance of the fixtures can be obtained from the experience of engineers. Thus, assuming that the FLE follows a normal distribution (Zhang and Shi 2016), the mean and standard variation of the normal distribution are set as 0.5 and 0.1, respectively.

The FEA model of parts I and II is established in ABAQUS, as shown in Figure 8. The mesh size for the parts is $100 \times 100 \times 6$ mm^3. After meshing, part I consists of 2255 S4R elements and 15 S3 elements, which indicates that the total number of nodes is $m_1 = 2343$. Part II is composed of 330 S4R elements, and the total number of nodes is $m_2 = 392$. The direction of gravity is set in the negative direction of the z-coordinate, and gravity is uniformly loaded on all parts. After establishing the FEA model, $\mathbf{K}$ and $\mathbf{f}$, used for calculating the nodal displacements, are exported.

Then, the CMINP model is established and solved by applying the NSGA-II-LHS method to find the optimal design of the fixture layout. The parameters of Algorithm 1 in Section 4.2 are set as

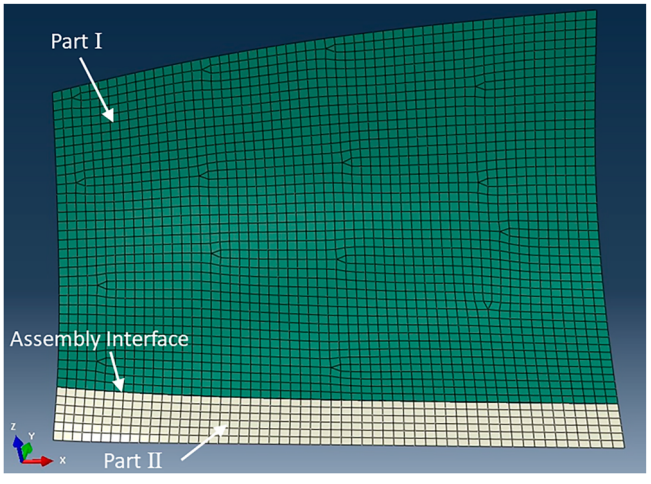

Figure 8. Finite element analysis (FEA) model of the compliant parts to be assembled.

$N = 30$, $L = 1300$, $Maxgen = 40$. Notably, the number of fixtures (N) is taken from the practical data obtained from engineering domain experience.

5.2. Results of fixture layout optimization

There are $m_0 = 56$ nodes along the assembly edge of each part. Each node has $df = 6$ degrees of freedom. The number of nodal displacements on parts I and II is $n_1 = 14058$ and $n_2 = 2352$, respectively. The precision requirement of the surface profile tolerance for each node is set as $\varepsilon = 3$. Fixtures cannot be placed on the four edges of the part, considering the actual production conditions. Thus, there are $\bar{m}_1^{\mathrm{F}} = 189$ and $\bar{m}_2^{\mathrm{F}} = 122$ infeasible nodes on parts I and II, respectively. Then, $N = 30$ nodal points are chosen from $m - \bar{m}_1^{\mathrm{F}} - \bar{m}_2^{\mathrm{F}} = 2424$ feasible nodes to support two curved panels. Finally, formula (13) is established to the optimal fixture layout for this case study.

Given the objectives and constraints described in Section 3, the NSGA-II-LHS method is used to achieve the optimal design of the fixture layout. The optimization process is repeated 10 times with the same parameters mentioned in Section 5.1. The anchor point, utopia point and best-compromised point are important terms, which represent the best point of each objective function, the intersection of the minimum of both objective functions and the corresponding Pareto solution lying as close as possible to the utopia point, respectively (Halim, Ismail, and Das 2021). The specific values of utopia points and best-compromised points are presented in Table 2.

The mean and variance values of utopia points for the corresponding problem experiment are (0.2150, 0.1170) and (0.0012, 0.0021), while the mean and variance values of best-compromised points are (0.3280, 0.3050) and (0.0015, 0.0063). Therefore, the utopia points and best-compromised points of 10-run solutions are stable. Run 7 is selected as the final result owing to the better values of objective functions. The Pareto-optimal solutions of Run 7 are illustrated in Figure 9. Point A in

Table 2. Utopia point and best-compromised point of all experiments.

No.	Utopia point	Best-compromised point	No.	Utopia point	Best-compromised point
Run 1	(0.17, 0.11)	(0.36, 0.22)	Run 6	(0.22, 0.10)	(0.35, 0.33)
Run 2	(0.26, 0.11)	(0.32, 0.26)	Run 7	(0.18, 0.08)	(0.26, 0.28)
Run 3	(0.17, 0.12)	(0.36, 0.22)	Run 8	(0.20, 0.24)	(0.30, 0.43)
Run 4	(0.22, 0.08)	(0.28, 0.39)	Run 9	(0.24, 0.10)	(0.35, 0.41)
Run 5	(0.26, 0.11)	(0.32, 0.26)	Run 10	(0.23, 0.12)	(0.38, 0.25)

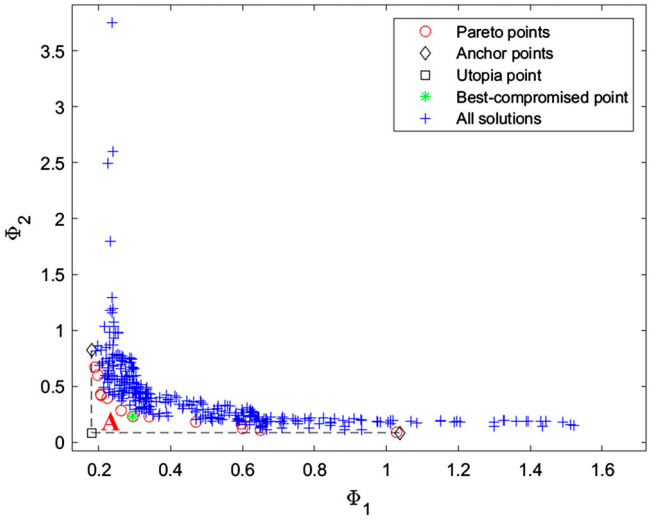

Figure 9. Pareto-optimal solutions calculated by the butt clearance control-oriented fixture layout optimization (BCCFLO) method.

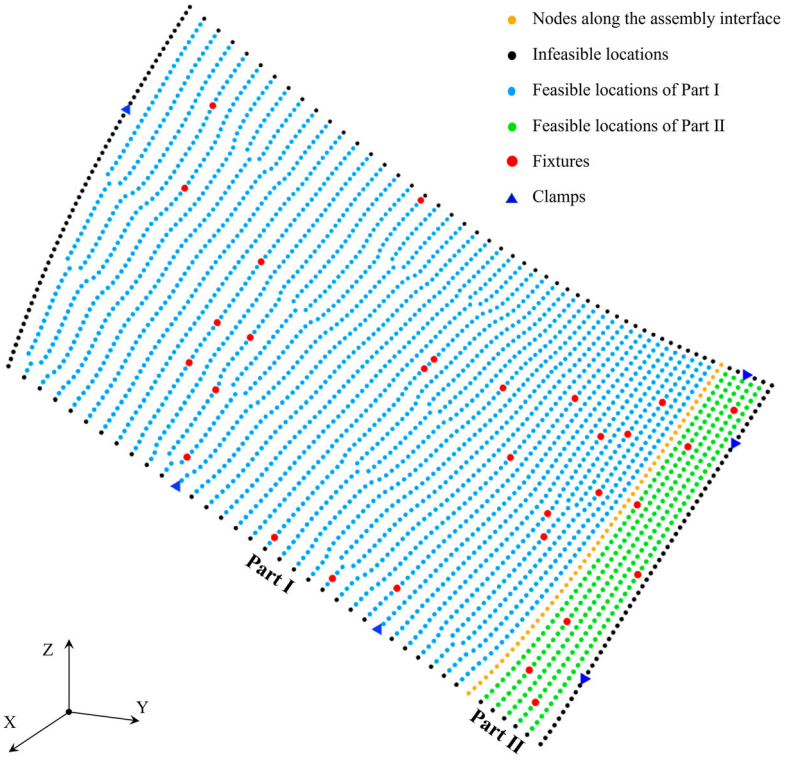

Figure 10. Positions of feasible, infeasible nodes, six clamps of two parts and the proposed fixture layout.

Figure 9 is the best-compromised point, which is selected as the optimal solution for the fixture layout design.

The mean, maximum and variance of the assembly clearance dimensions are then introduced to quantitatively compare the proposed optimal fixture layout (Figure 10) with current practice (Figure 11). The comparison results of the two fixture layouts are summarized in Table 3. It can be seen that the optimal fixture layout of the BCCFLO method significantly reduces the mean, maximum and variance of the assembly clearance dimensions, by 94.43%, 92.31% and 99.98%, respectively. In addition, Table 3 shows that the optimal fixture layout achieves 65.62% less maximum displacement of two compliant parts.

To further compare the results of the BCCFLO method and the current practice, the part deformation of two curved panels is presented in Figure 12. The part deformation in the x-, y- and z-directions is shown in Figure 12(a)–(c), respectively. The colour interval indicates the deformation difference, and larger colour intervals indicate large deformation differences. As shown in Figure 12, the larger dimensional gaps that exist in the result of the current practice are marked. In contrast to the current practice, the deformation colour interval of the BCCFLO method is smaller between the butt clearance of the two parts. The deformation colour is more consistent along the assembly interface, thereby indicating that the optimal fixture layout has smaller and straighter butt clearance along the assembly interface.

In this case study, the central processing unit (CPU) time is 9407.39 s, *i.e.* 2.61 h, on a desktop with an Intel® Core™ i9-13900 K 3.00 GHz processor and 32 GB of RAM. It satisfies the practice requirement because the fixture layout optimization is accomplished in the design phase. Besides, the method proposed to calculate the part deformation under various fixture layouts is a physical model based on the FEE, which avoids a large number of simulation calculations. Thus, integrating

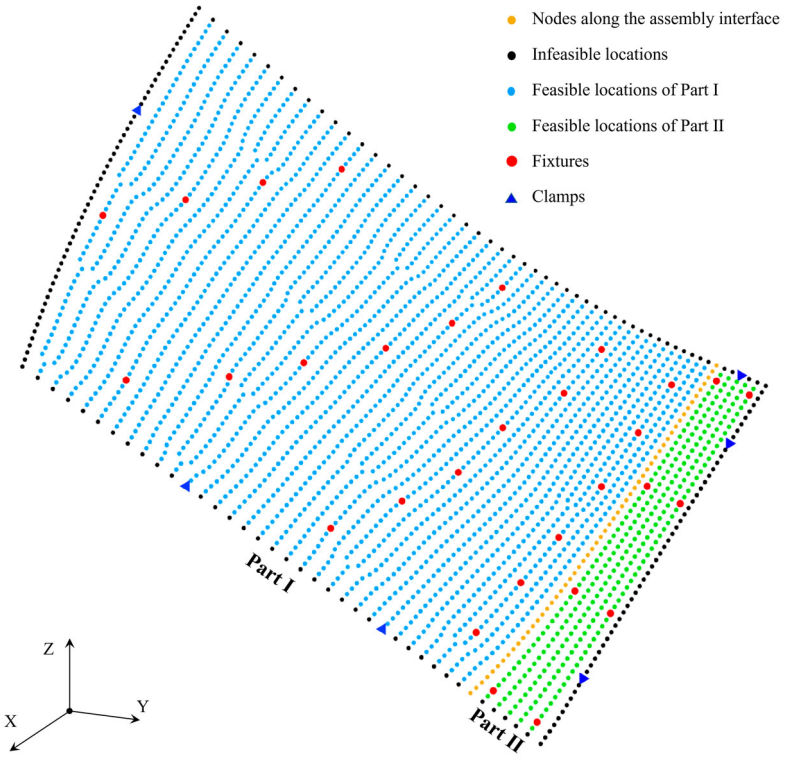

Figure 11. Positions of feasible, infeasible nodes, six clamps of two parts and current practice.

Table 3. Comparisons between the butt clearance control-oriented fixture layout optimization (BCCFLO) method and current practice (mm).

Methods	Mean gap	Max. gap	Variance of gap	Max. displacement
BCCFLO method	0.26	0.62	0.28	2.85
Current practice	4.67	8.06	117.86	8.29
Reduction percentage	94.43%	92.31%	99.98%	65.62%

the proposed method with adjustable fixtures is efficient for the shipbuilding industry to control the butt clearance between compliant parts to be assembled.

5.3. Comparison and validation

The performance of the BCCFLO method using the NSGA-II-LHS algorithm is compared with that using the traditional NSGA-II algorithm. The model parameters of the traditional NSGA-II algorithm are the same as the settings in Section 5.1. Figure 13(a) and (b) report the Pareto-optimal solutions calculated by the NSGA-II-LHS and NSGA-II algorithms, respectively. As shown in Table 4, the anchor point, utopia point, closeness and best-compromised candidate of the NSGA-II-LHS are smaller than those of the NSGA-II.

The BCCFLO method in this article is also compared with the method integrating the direct stiffness method and stochastic optimization (DSMSO) (Du *et al.* 2021). The butt clearances under different fixture layouts from the BCCFLO method using NSGA-II-LHS or NSGA-II, the DSMSO method and the current practice are illustrated in Figure 14. The butt clearance under fixture layouts calculated by the BCCFLO method using NSGA-II-LHS are reduced significantly compared to other

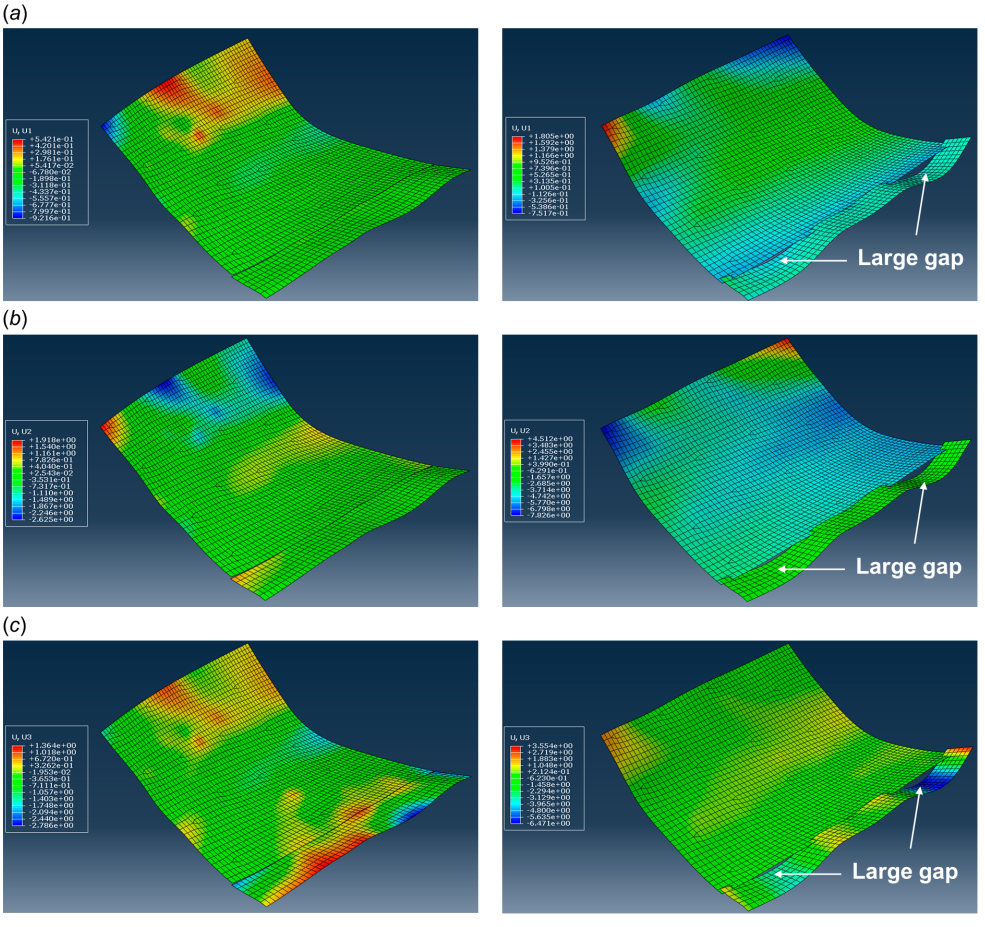

Figure 12. Part deformation of the butt clearance control-oriented fixture layout optimization (BCCFLO) method (left) and current practice (right) in the (a) *x*-direction, (b) *y*-direction, and (c) *z*-direction.

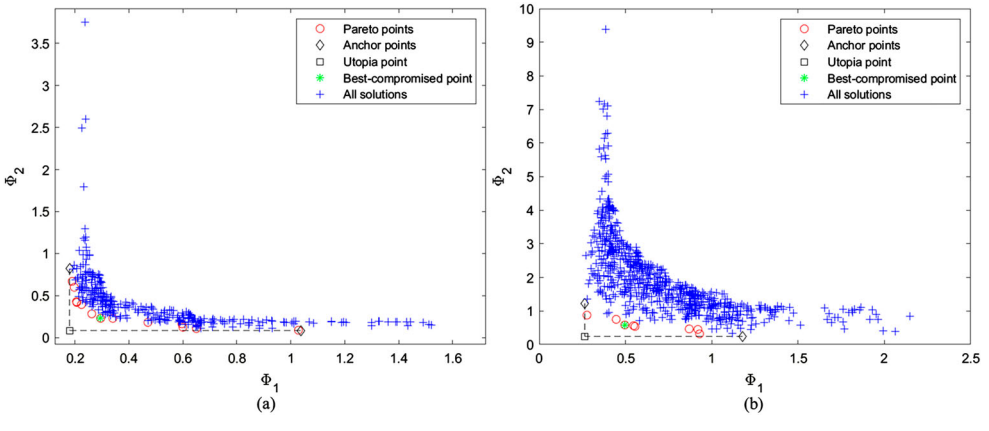

Figure 13. Pareto-optimal solutions calculated by (a) non-dominated sorting genetic algorithm-II based on Latin hypercube sampling (NSGA-II-LHS); and (b) non-dominated sorting genetic algorithm-II (NSGA-II).

Table 4. Comparisons of Pareto-optimal solutions between the non-dominated sorting genetic algorithm-II based on Latin hypercube sampling (NSGA-II-LHS) and non-dominated sorting genetic algorithm-II (NSGA-II) (mm).

	Anchor point	Utopia point	Closeness	Best-compromised candidate
NSGA-II-LHS	(0.18, 1.04); (0.82, 0.08)	(0.18, 0.08)	0.19	(0.26, 0.28)
NSGA-II	(0.26, 1.18); (1.23, 0.24)	(0.26, 0.24)	0.41	(0.50, 0.58)

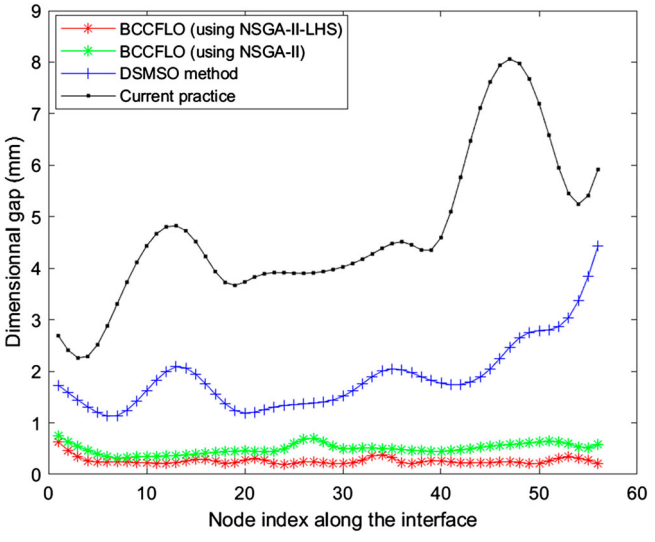

Figure 14. Dimensional gaps of fixture layouts calculated by different methods: butt clearance control-oriented fixture layout optimization (BCCFLO) using the non-dominated sorting genetic algorithm-II based on Latin hypercube sampling (NSGA-II-LHS), BCCFLO using the non-dominated sorting genetic algorithm-II (NSGA-II), direct stiffness method and stochastic optimization (DSMSO), and current practice.

Table 5. Comparisons of dimensional gaps under fixture layouts from different methods (mm).

	Mean gap	Max. gap	Variance of gap
Current practice	4.68	8.06	117.86
DSMSO	1.89	4.43	26.17
BCCFLO (using NSGA-II)	0.50	0.75	0.58
BCCFLO (using NSGA-II-LHS)	0.26	0.62	0.28

Note: DSMSO = direct stiffness method and stochastic optimization; BCCFLO = butt clearance control-oriented fixture layout optimization; NSGA-II = non-dominated sorting genetic algorithm-II; NSGA-II-LHS = non-dominated sorting genetic algorithm-II based on Latin hypercube sampling.

methods, which demonstrate the superiority of the BCCFLO method. Furthermore, Table 5 gives the mean, maximum and variance of dimensional gaps along the assembly clearance under fixture layouts calculated by different methods. The results show the superior performance of the proposed BCCFLO method using the NSGA-II-LHS in comparison with other methods.

To further validate the superiority of the BCCFLO method compared with the current practice, the deformation scale factor is set to 30 to show the butt clearance of two compliant parts in detail. The FEA simulation results of the BCCFLO method and the current practice are shown in Figure 15.

As shown in Figure 15(a), the butt clearance under the proposed fixture layout design is straighter and controlled below 1 mm. However, the butt clearance under the current practice presented in Figure 15(b) shows an increasing trend, with two dramatic increases at the left end and the right end. Therefore, the proposed method is superior to the current practice in minimizing and straightening the assembly clearance.

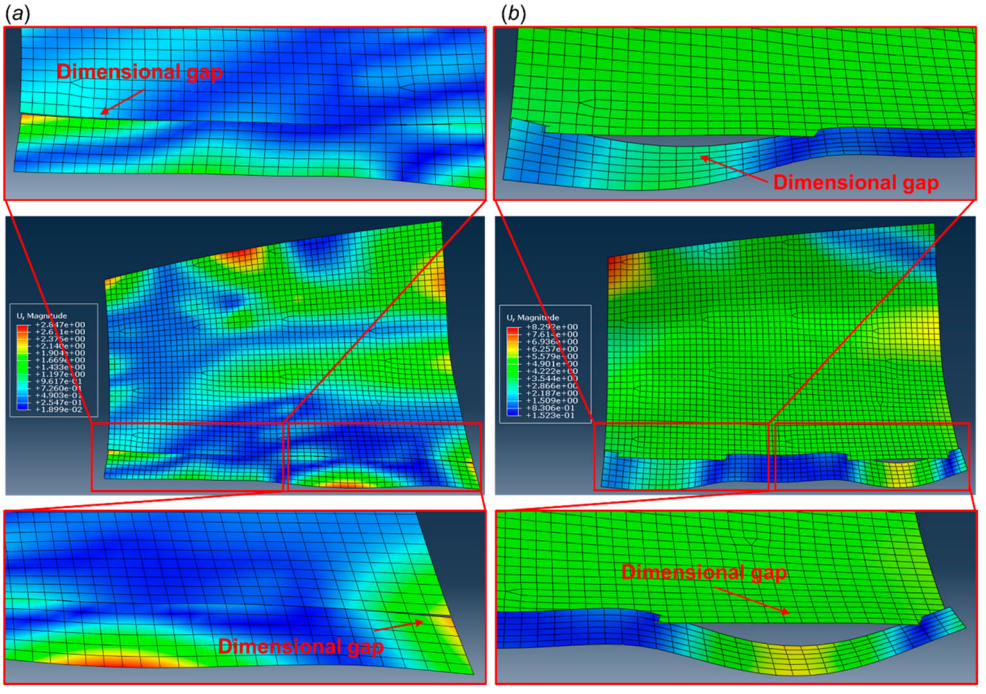

Figure 15. Butt clearance under (a) butt clearance control-oriented fixture layout optimization (BCCFLO) method and (b) current practice.

Table 6. Linear displacement differences between the finite element equation considering fixture layout and fixture locating error (FEE-FLE) and Monte Carlo simulation (MCS) (mm).

Linear displacement	Maximum absolute difference	Mean absolute difference
Displacement in the *x*-direction of node 55	4.24×10^{-4}	4.24×10^{-4}
Displacement in the *y*-direction of node 55	1.66×10^{-3}	1.66×10^{-3}
Displacement in the *z*-direction of node 55	8.86×10^{-5}	8.86×10^{-5}
Displacement in the *x*-direction of node 2	1.17×10^{-4}	1.17×10^{-4}
Displacement in the *y*-direction of node 2	1.13×10^{-3}	1.13×10^{-3}
Displacement in the *z*-direction of node 2	7.04×10^{-4}	7.04×10^{-4}
Nodal displacement of each node on part I	3.14×10^{-3}	8.77×10^{-4}
Nodal displacement of each node on part II	1.11×10^{-2}	2.80×10^{-3}

To validate the accuracy of part variations calculated by the FEE-FLE, the results of nodal displacements obtained using the FEE-FLE are compared with those of the Monte Carlo simulation (MCS). The FLE of each fixture is generated by MATLAB, which follows a normal distribution as described in Section 5.1. The MCS is performed 100 times by running the finite element model in ABAQUS. The nodes along the assembly interface, such as node 55 on part I and node 2 on part II, are selected, and their linear displacements in the *x*-, *y*- and *z*-directions are obtained using both the FEE-FLE and MCS. The maximum and mean linear displacement differences of parts I and II calculated by FEE-FLE and MCS are presented in Table 6.

The results of the FEE-FLE are highly consistent with those of the MCS. The differences in linear displacement calculated by the two methods are small, which meets the accuracy requirement. Thus, the proposed method has a notable advantage that can realize accurate calculation of nodal displacements considering the FLE during the optimization process without requiring intensive FEA simulations using commercial software or establishing surrogate models.

6. Conclusions and future work

This article develops a new method called BCCFLO to optimize the fixture layout for large compliant parts. Owing to the compliant nature and large dimensions of ship parts, and unavoidable fixture locating errors, the part deformation is large, which results in poor butt clearance between the parts to be assembled. Therefore, it is an important and challenging task to achieve the optimal fixture layout to control the butt clearance while considering the fixture locating error. To address this challenge, a CMINP problem based on the proposed FEE-FLE is established. To solve this problem, the NSGA-II-LHS method is further developed to find the optimal fixture layout.

Furthermore, the application of the proposed BCCFLO method is illustrated with a case of large compliant part assembly in the shipbuilding industry, providing comparisons and analyses of different methods. The results demonstrate that the proposed method is consistent with the simulation validation, satisfies the requirements of practical application, and outperforms the other methods in terms of the mean, maximum and variance of the assembly clearance.

Future work will be conducted on the optimal and robust design of the fixture layout for a product family. Optimizing the number of fixtures and fixture layout simultaneously is another meaningful direction for future work.

Acknowledgements

This research is supported by the National Key Research and Development Program of China [2022YFF0605700], National Natural Science Foundation of China [51875359 and 72001139], Natural Science Foundation of Shanghai [20ZR1428600], CSSC-SJTU Marine Equipment Forward Looking Innovation Foundation [22B010432] and Oceanic Interdisciplinary Program of Shanghai Jiao Tong University [SL2021MS008].

Disclosure statement

No potential conflict of interest was reported by the authors.

Funding

This work was supported by the National Key Research and Development Program of China [grant number 2022YFF0605700]; National Natural Science Foundation of China [grant number 51875359]; Natural Science Foundation of Shanghai Municipality [grant number 20ZR1428600]; CSSC-SJTU Marine Equipment Forward Looking Innovation Foundation [grant number 22B010432]; Oceanic Interdisciplinary Program of Shanghai Jiao Tong University [grant number SL2021MS008].

Data availability statement

The authors confirm that the data supporting the findings of this study are available within the article.

References

Butt, S. U., M. Arshad, A. A. Baqai, H. A. Saeed, N. A. Din, and R. A. Khan. 2021. "Locator Placement Optimization for Minimum Part Positioning Error During Machining Operation Using Genetic Algorithm." *International Journal of Precision Engineering and Manufacturing* 22 (5): 813–829. https://doi.org/10.1007/s12541-021-00500-6.

Cai, W., S. J. Hu, and J. X. Yuan. 1996. "Deformable Sheet Metal Fixturing: Principles, Algorithms, and Simulations." *Journal of Manufacturing Science and Engineering* 118 (3): 318–324. https://doi.org/10.1115/1.2831031.

Camelio, J. A., S. J. Hu, and D. J. Ceglarek. 2004. "Impact of Fixture Design on Sheet Metal Assembly Variation." *Journal of Manufacturing Systems* 23 (3): 182–193. https://doi.org/10.1016/S0278-6125(05)00006-3.

Camelio, J. A., S. J. Hu, and S. P. Marin. 2004. "Compliant Assembly Variation Analysis Using Component Geometric Covariance." *Journal of Manufacturing Science and Engineering* 126 (2): 355–360. https://doi.org/10.1115/1.1644553.

Chan, K. C., and H. Tansri. 1994. "A Study of Genetic Crossover Operations on the Facilities Layout Problem." *Computers & Industrial Engineering* 26 (3): 537–550. https://doi.org/10.1016/0360-8352(94)90049-3.

Chen, B. Q., and C. Guedes Soares. 2016. "Effects of Plate Configurations on the Weld Induced Deformations and Strength of Fillet-Welded Plates." *Marine Structures* 50: 243–259. https://doi.org/10.1016/j.marstruc.2016.09.004

Deb, K., A. Pratap, S. Agarwal, and T. A. M. T. Meyarivan. 2002. "A Fast and Elitist Multiobjective Genetic Algorithm: NSGA-II." *IEEE Transactions on Evolutionary Computation* 6 (2): 182–197. https://doi.org/10.1109/4235.996017.

Du, J., C. Liu, J. Liu, Y. Zhang, and J. Shi. 2021. "Optimal Design of Fixture Layout for Compliant Part with Application in Ship Curved Panel Assembly." *Journal of Manufacturing Science and Engineering* 143 (6): 061007. https://doi.org/10.1115/1.4048954.

Eyres, D. J., and G. J. Bruce. 2012. *Ship Construction*. Burlington, MA: Butterworth-Heinemann.

Halim, A. H., I. Ismail, and S. Das. 2021. "Performance Assessment of the Metaheuristic Optimization Algorithms: An Exhaustive Review." *Artificial Intelligence Review* 54 (3): 2323–2409. https://doi.org/10.1007/s10462-020-09906-6.

Kaya, N. 2006. "Machining Fixture Locating and Clamping Position Optimization Using Genetic Algorithms." *Computers in Industry* 57 (2): 112–120. https://doi.org/10.1016/j.compind.2005.05.001.

Kim, P., and Y. Ding. 2004. "Optimal Design of Fixture Layout in Multistation Assembly Processes." *IEEE Transactions on Automation Science and Engineering* 1 (2): 133–145. https://doi.org/10.1109/TASE.2004.835570.

Li, Z., L. E. Izquierdo, M. Kokkolaras, S. J. Hu, and P. Y. Papalambros. 2008. "Multiobjective Optimization for Integrated Tolerance Allocation and Fixture Layout Design in Multistation Assembly." *Journal of Manufacturing Science and Engineering* 130 (4): 044501. https://doi.org/10.1115/1.2951951.

Liu, C., J. Liu, Y. Zhang, S. Jin, C. Wang, and X. Lai. 2020. "Study on the Propagation of Dimensional Deviation in the Hull Block Building Process." *Journal of Ship Production and Design* 36 (2): 143–151. https://doi.org/10.5957/jspd.2020.36.2.143.

McKay, M. D., R. J. Beckman, and W. J. Conover. 2000. "A Comparison of Three Methods for Selecting Values of Input Variables in the Analysis of Output from a Computer Code." *Technometrics* 42 (1): 55–61. https://doi.org/10.1080/00401706.2000.10485979.

Phoomboplab, T., and D. Ceglarek. 2008. "Process Yield Improvement Through Optimum Design of Fixture Layouts in 3D Multistation Assembly Systems." *Journal of Manufacturing Science and Engineering* 130 (6): 061005. https://doi.org/10.1115/1.2977826.

Rong, Y., W. Hu, Y. Kang, Y. Zhang, and D. W. Yen. 2001. "Locating Error Analysis and Tolerance Assignment for Computer-Aided Fixture Design." *International Journal of Production Research* 39 (15): 3529–3545. https://doi.org/10.1080/00207540110056243.

Shen, Y., R. Wang, M. Liu, Y. Wang, M. Chen, Y. Zhao, and H. Zhou. 2020. "Research on Development and key Technologies of Intelligent bed-jig System for Ship Sectional Construction." *IOP Conference Series: Materials Science and Engineering* 831 (1): 012014. https://doi.org/10.1088/1757-899X/831/1/012014.

Shojaeefard, M. H., A. Khalkhali, H. Faghihian, and M. Dahmardeh. 2018. "Optimal Platform Design Using non-Dominated Sorting Genetic Algorithm II and Technique for Order of Preference by Similarity to Ideal Solution; Application to Automotive Suspension System." *Engineering Optimization* 50 (3): 471–482. https://doi.org/10.1080/0305215X.2017.1324853.

Tian, Z. Q., X. M. Lai, and Z. Q. Lin. 2009. "Robust Fixture Layout Design for Multi-station Sheet Metal Assembly Processes Using a Genetic Algorithm." *International Journal of Production Research* 47 (21): 6159–6176. https://doi.org/10.1080/00207540802178091.

Vishnupriyan, S., M. C. Majumder, and K. P. Ramachandran. 2011. "Optimal Fixture Parameters Considering Locator Errors." *International Journal of Production Research* 49 (21): 6343–6361. https://doi.org/10.1080/00207543.2010.532167.

Xie, W., Z. Deng, B. Ding, and H. Kuang. 2015. "Fixture Layout Optimization in Multi-station Assembly Processes Using Augmented ant Colony Algorithm." *Journal of Manufacturing Systems* 37: 277–289. https://doi.org/10.1016/j.jmsy.2014.08.005.

Xing, Y. 2017. "Fixture Layout Design of Sheet Metal Parts Based on Global Optimization Algorithms." *Journal of Manufacturing Science and Engineering* 139 (10): 101004. https://doi.org/10.1115/1.4037106.

Xu, X., Y. Jiang, and H. Pueh Lee. 2017. "Multi-objective Optimal Design of Sandwich Panels Using a Genetic Algorithm." *Engineering Optimization* 49 (10): 1665–1684. https://doi.org/10.1080/0305215X.2016.1265304.

Yang, B., Z. Wang, Y. Yang, Y. Kang, and X. Li. 2017. "Optimum Fixture Locating Layout for Sheet Metal Part by Integrating Kriging with Cuckoo Search Algorithm." *The International Journal of Advanced Manufacturing Technology* 91 (1–4): 327–340. https://doi.org/10.1007/s00170-016-9638-5.

Zhang, T., and J. Shi. 2016. "Stream of Variation Modeling and Analysis for Compliant Composite Part Assembly—Part I: Single-Station Processes." *Journal of Manufacturing Science and Engineering* 138 (12): 121003. https://doi.org/10.1115/1.4033231.